LA-UR- 00-31

Approved for public release; distribution is unlimited.

Title:	STATISTICAL ANALYSIS ON TURBULENT PREMIXED FLAME WITH A CYCONE-JET COMBUSTOR
Author(s):	K. Yamamoto
Submitted to:	Twenty Eight International Symposium on Combustion, University of Edinburgh, Scotland, held on July 30th - August 4, 2000.

Los Alamos
NATIONAL LABORATORY

Form 836 (10/96)

DISCLAIMER

Statistical Analysis on Turbulent Premixed Flame with a Cyclone-jet Combustor

by

K. Yamamoto, Y. Nishizawa, and Y. Onuma
Department of Mechanical Engineering, Toyohashi University of Technology
1-1 Hibarigaoka, Tempaku, Toyohashi-shi, Aichi 441-8580, JAPAN

Correspondence: Kazuhiro YAMAMOTO (Visiting Researcher at LANL)
Los Alamos National Laboratory
Attention: Kazuhiro Yamamoto, ATW
MS H854, Los Alamos, NM 87545
Tel. 505-665-6840
Fax. 505-665-6927
E-mail: kazuhiro@lanl.gov

Word Count: Text (Introduction – References) 3233

Figures (8 Figures)	2200 (400x3 (Figs. 2, 4, 5), 200x5)
Equations (2×21)	42
Total	5475

Presentation: Oral presentation
Colloquium: Turbulent Premixed and Partially Premixed Combustion

Statistical Analysis on Turbulent Premixed Flame with a Cyclone-jet Combustor

by

K. Yamamoto, Y. Nishizawa, and Y. Onuma
Department of Mechanical Engineering, Toyohashi University of Technology
1-1 Hibarigaoka, Tempaku, Toyohashi-shi, Aichi 441-8580, JAPAN

(ABSTRACT)

To investigate the premixed flame structure in highly turbulent flow, we have used a cyclone-jet combustor, which stabilizes the premixed flames over a wide range of turbulent properties. With Mie scattering imaging, we have obtained tomographic flame images to visualize the flame structure. The local flame characteristics have been examined with an electrostatic probe. The new approach has been proposed to determine statistically the reaction zone thickness based on probability of reaction zone existing. By this method, we can estimate the turbulent flame thickness qualitatively. From the tomographic images, when the turbulence is relatively low, one continuous flame sheet wrinkles and a typical wrinkled laminar flame is formed. As the exit velocity is further increased, the flame wrinkling is increased, but the size of its wrinkles becomes smaller with many cusps on the flame front. In signal waveform of ion current, the fluctuation of ion current increases. When the velocity exceeds 30 m/s, one continuous flame sheet cannot be sustained and PDF of ion current becomes the so-called normal distribution (Gaussian distribution) due to the random peak value of ion current. In addition, the statistically obtained reaction zone thickness becomes wider. Although these results are not conclusive evidence of distributed reaction combustion, it seems that, based on the statistically analyzed flame characteristics, the destruction of laminar flame structure occurs in highly turbulent combustion and thickened flame structure appears.

INTRODUCTION

For modeling turbulent combustion, numerous studies have been made [1-16]. In these studies, several different flame regimes have been proposed to classify the flame structure with phase diagram [5,6]. It is considered that if the smallest turbulent eddies have a size below the reaction zone thickness, these eddies might penetrate into the reaction zone to form thickened flame with distributed reaction zone [1-6]. As a limit between so called flamelet regime with thin wrinkled flame fronts and distributed combustion regime with thickened flame fronts, the Klimov-Williams criterion has been proposed. However, some recent studies have pointed out the persistence of laminar-like flame structure even under highly turbulent conditions [12-14]. In the work of Buschmann et al. [15], it has been found that thermal flame-front structure is significantly thinned compared with that of the laminar flame, which is contrary to the expectation of thickened flames. Mansour et al. [16] have observed thin reaction zone with relatively thick preheat zone in simultaneous two-dimensional CH-LIF/Rayleigh measurements. Thus, the premixed turbulent flame structure has not been clearly understood, and a new phase diagram may be needed to construct turbulent combustion regimes.

In our previous studies, with a cyclone-jet combustor, we have investigated turbulent flame structure over a wide range of turbulent intensities, with u'/S_L exceeding 10 in a stationary jet flame [17,18]. We have observed the flame behavior with CCD camera and high-speed video camera. Temperature measurement has been conducted with a compensated thermocouple. In relatively weak turbulent flow, the wrinkled laminar flame is formed. When the velocity exceeds 20-30 m/s, one continuous flame sheet is not observed and the PDF of temperature is no longer bimodal, which is the typical thermal structure of the wrinkled laminar flame. Although there are certain inherent uncertainties in temperature measurement, it could be considered that, in highly turbulent flow, the destruction of laminar flame structure occurs due to the turbulent motion.

For the conclusive discussion, we need further studies to detect the local flame structure with diagnostics of high spatial or temporal resolution. We use an electrostatic probe to characterize the flame structure, which has high time resolution (10^{-7} ~ 10^{-8} s [19]) enough to follow the flame fluctuation even under highly turbulent conditions. Normally, since the reaction zone fluctuates strongly in turbulent flow and its thickness is less than 1 mm, it is difficult to measure the reaction zone thickness. In this study, we propose the new approach to determine statistically the reaction zone thickness based on probability of reaction zone existing. By this method, we can estimate the turbulent flame thickness qualitatively and verify the Klimov-Williams criterion. Also, by sheet laser tomography, the instantaneous flame structure is investigated.

EXPERIMENTAL

Figure 1 shows a cyclone-jet combustor used in this study. It consists of a combustion chamber with a main jet nozzle and two cyclone nozzles for pilot flames, which stabilizes the turbulent flames. The diameter of the main jet nozzle, d, is 13 mm. The cyclone combustor is of 21 mm i.d. and 23 mm height, with two cyclone nozzles of 2.4 mm i.d.. The fuel is propane. In the experiment, we vary the mean velocity of the main jet, U_m, and the equivalence ratio of the mixture, ϕ_m, with a fixed condition of pilot flames for U_p = 20 m/s and ϕ_p = 0.7.

To obtain the instantaneous flame structure, we use laser tomography. A Nd:YAG laser (Spectra-physics GCR-170) operating at ca. 450 mJ/pulse is used to produce laser sheet of 300μm thickness. The duration of laser pulse is 6 ns. MgO particles are used as seeding particles [18]. The Mie scattering image is recorded by a still camera.

A micro-electrostatic probe is used to collect the information on local flame structure. It

specifies the reaction region of high ion concentration where the ion-electron formation and recombination reactions occur. It consists of a platinum wire sensor of 0.1 mm in diameter and 0.5 mm long. The sensor projected from a fine quartz tube over which a water-cooled stainless tube is fitted to prevent the quartz tube from the thermal dielectric breakdown. The potential drop across the load resistance is amplified to obtain ion currents, which is stored in the computer.

RESULTS AND DISCUSSIONS

Appearance of Flames

Figure 2(a) shows a direct photograph of a flame stabilized in a cyclone-jet combustor for U_m = 10 m/s and ϕ_p = 0.75. The exposure time is about 0.01 s. Here, Z represents the axial distance from the exit of the combustor. It is the turbulent jet flame, although the instantaneous flame structure is not clear.

Figure 2(b) shows the tomographic image. In previous study, we have found that there are three regions in the image [18]. The first region is that of high intensity of scattering, which indicates unburned gas region of low temperature. The second region is that of low intensity of scattering, which is burned gas region of high temperature. The third is surrounding air of no scattering. As seen in this picture, the flame has one continuous flame front with many cusps, which seems to be a so-called wrinkled laminar flame.

Figure 2(c) shows the axial distribution of mean ion current obtained along the center axis. The region of high ion current corresponds to the reaction region where hydrocarbon-oxygen combustion reaction occurs [8]. It is found that the region of high ion concentration exists around Z = 50~100 mm, which means that the flame is fluctuating. Next, we obtain the tomographic

images with changing the exit velocity.

Figure 3 shows the enlarged tomographic images of flames for U_m = 10, 15, and 30 m/s, φ_m = 0.75. The scale is approximately 75 cm from top to bottom of the image. It is found that, when the exit velocity is relatively low (U_m = 10 m/s), there is a continuous flame surface with wrinkles. As the exit velocity is further increased to U_m = 15 m/s, the flame wrinkling increases and there are many cusps on the flame front. However, over 20~30 m/s, the flame structure largely changes. As seen in Fig. 3(c), it is difficult to distinguish between regions of unburned and burned gases on the basis of the intensity of scattering. This indicates that the wrinkled laminar flame structure does not exist, which is supported by the previous temperature measurements [18].

Signal Waveform of Ion Current

Next, we measure the ion currents to investigate the local flame structure. When the electrostatic probe is passed across the flame, the ion current starts to increase as a measuring point approaches the visible flame zone, and it reaches a maximum inside the reaction zone, then it decreases on the burned gas side. As already pointed out [8], the ion current in the burned gas is relatively high due to the slow recombination reaction. Therefore, from the signals of the ion probe, we could know the flame motion. Figure 4 shows the signal waveforms of ion currents for U_m =10, 15, and 30 m/s. We compare the profiles at the position where the mean ion current takes maximum in the axial distribution. Based on the previous velocity measurement in cold flow [18], the Karlovitz number (Ka) of these conditions are calculated to be 0.81, 1.78, and 3.37, respectively. It is found that, as the exit velocity is increased, the flame fluctuation is increased.

In Fig. 4 (c), for U_m = 30 m/s, blob-like structures with multiple peaks appear.

Yoshida et al. [7,9], also examined the flame structure in highly turbulent flow by using an opposed jet burner. It has been pointed out that, such blocks with multiple ion peaks appear when the turbulence is very high, which may indicate the existence of flames with distributed reaction zone consisting of the small eddies of completely burned and partially reacting gases. Thus, this flame structure may appear in Fig. 4(c). To further characterize the flame structure, we obtained the PDF of ion currents.

PDF of Ion Current

Figure 5 shows the PDF profiles of flames in Fig. 4, which are obtained based on 65,000 data points. The number at the left corner is the probability of zero in current. For U_m = 10 m/s, the probability of zero ion current is relatively high, and it monotonically decreases as the ion currents is increased. It is well known that, when the turbulence is relatively weak, a so-called wrinkled laminar is formed and the PDF of temperature shows a bimodal shape, where low and high peak temperatures correspond to those of the unburned and burned gases [18]. However, its PDF of ion current must not be bimodal, because the ion concentration is high only in the thin reaction zone, and the ion current is low in the unburned or burned gas region. Thus, even if the probe is inserted at the position where the reaction often occurs, the flame is fluctuated rapidly due to turbulence and the unburned and burned gases also appear, so that the PDF of low ion current becomes high. It is considered that Fig. 5 (a) is a typical PDF profile of the wrinkled laminar flame. The PDF profile for U_m = 15 m/s is similar, although the probability of low ion current is lower.

However, as the exit velocity is further increased, the PDF profile changes. For U_m = 30 m/s,

the PDF profile is similar to a so called normal distribution (Gaussian distribution), which may be caused by the fact that there exits partially reacting gases and the peak value in the signal waveform of ion currents becomes random. From these PDF profiles, it is found that the flame structure changes with turbulence.

Probability of Reaction Zone Existing and Statistically Obtained Reaction Zone Thickness

It should be noted that the ion current collected by an electrostatic probe depends on the flow velocity and flame curvature, and it difficult to understand the combustion condition based on the ion current signals [19]. However, at least, we can specify the reaction zone by examining the region of high ion concentration where hydrocarbon-oxygen combustion reaction occurs. Here, we propose a new statistic approach to determine statistically the reaction zone thickness based on ion current signals. By this method, we can investigate the variations of the reaction zone thickness with turbulence qualitatively.

At first, to distinguish whether the reaction occurs or not at the specified space and time, we use simple threshold procedure. The ion current signals are binarized with reaction variable whose value is unity or zero. This procedure is shown in Fig. 6. If the ion current is higher than a threshold, there occurs reaction and the reaction variable, a, is unity, whereas if the ion current is lower than this threshold, a is zero. According to Furukawa et al. [19], the peak ion current across the flame depends on the angle between the flame and the sensor of the ion probe. It takes maximum when the flame surface is parallel to the sensor. The reduced peak value means the lower spatial resolution when the same reaction zone passes the sensor, which is larger than the diameter of ion probe. We adopted the half value of maximum ion current as threshold, I_{th}, because the width of half height is considered to be the time when the reaction zone passes the

sensor. It should be noted that, as seen in Fig. 6, we only consider the peaks when the flame passes the sensor parallel to it to avoid obtaining thickened flame only due to the lower spatial resolution. To confirm the validity of our method, we compare the obtained reaction zone thickness with the theoretically expected value, Zeldovitch thickness [20].

Next, we obtain the mean value of a with time-averaging procedure, $p(x_i)$, which is considered to be the probability of reaction zone existing at specified location, x_i. Here, if we choose the coordinate normal to the (mean) flame surface, x^*, we can estimate the flame thickness. Let us consider the example. The flame is stationary and the reaction zone is located between $x^* = 0$ and $x^* = \delta$, where δ is the reaction zone thickness. The value of $p(x^*)$ is unity inside the reaction zone, and it is zero outside the reaction zone. If we integrate $p(x^*)$ along the coordinate of x^*, we can obtain the reaction zone thickness.

$$\int_{-\infty}^{+\infty} p(x^*)dx^* = \int_0^{\delta} p(x^*)dx^* = \int_0^{\delta} 1\ dx^* = \delta.$$

When the flame is wrinkled and is not stationary, the flame is moving and $p(x^*)$ has a value between zero and unity. In this case, correction of the flame thickness is needed, because the flame is always inclined to the mean flame front.

In Bray-Moss-Libby (BML) model [21], this inclination is called flamelet crossing angle, θ, which is defined as the acute angle between the mean progress variable contour and the normal to the instantaneous front surface (see Fig. 7). The progress variable within a certain range corresponds to the flame zone. Recently, Shy et al. [22] have investigated the flamelet statistics in isotropic turbulent flow, and has pointed out that the overall mean cosine value of θ is nearly 0.65. In this study, we correct the flame thickness with this value. Then, the reaction zone

thickness is obtained as follows:

$$\delta = \overline{\cos(\frac{\pi}{2}-\theta)\int_{-\infty}^{+\infty} p(x^*)dx^*} = \overline{\cos(\frac{\pi}{2}-\theta)}\ \delta^* = \overline{\sin\theta}\ \delta^* = \sqrt{1-(\overline{\cos\theta})^2}\ \delta^*.$$

It should be noted that the obtained reaction zone thickness is not instantaneous flame thickness but statistically expected value.

Figure 7 shows the radial distribution of probability of reaction zone existing for U_m = 15m/s, which is obtained at Z = 20 mm. As seen in Fig. 2, around Z = 20 mm, the flame front seems to be normal to the radial direction. We chose the radial direction as x^* coordinate. Results show that the reaction zone only at r = 6 ~ 10 mm, which means that the flame is fluctuating in this region.

Based on this profile, we integrate the probability of reaction zone existing along the radial direction to obtain the reaction zone thickness. Results are shown in Fig. 8. In this figure, Zeldovitch thickness, δ_z, is also shown, which is commonly defined as the reaction zone thickness. This thickness is obtained by $\delta_z \equiv \nu/S_L$ [20], where ν is the kinematic viscosity of the mixture and S_L is the laminar flame speed, which is obtained by Ref. 23.

Figure 8a shows the variations of reaction zone thickness with equivalence ratio, which is obtained at U_m = 5m/s, Z=10mm. We also obtained the reaction zone thickness of Bunsen flame (U = 1.8 m/s, ϕ = 0.85), which is formed in relatively weak turbulent flow. In the work of Chew et al. [24], the overall mean cosine value of θ is found to be 0.5 for Bunsen flame. It is found that the corrected reaction zone thickness of the Bunsen flame corresponds to the Zeldovich thickness, δ_z . Hence, by our proposed method, the reaction zone thickness can be obtained correctly. Also, as for the flames in the cyclone-jet combustor, its thickness is in good agreement with δ_z. Therefore, it is considered that their flame structures are similar to that of a laminar

flame and these flames are the wrinkled laminar flame. Next, we obtain the reaction zone thickness at Z = 20mm with changing the exit velocity. Results are shown in Fig. 8b. Equivalence ratio is fixed at 0.75. The calculated the Zeldovich thickness is 0.09mm.

As seen in this figure, it is found that, when the exit velocity is relatively low, the obtained reaction zone thickness is almost the same as Zeldovich thickness. However, it is interesting to note that, as the exit velocity is increased, the reaction zone thickness becomes larger. When the velocity is 30m/s, its thickness becomes almost twice. Thus, the flame in highly turbulent flow has statistically thicker reaction zone, which corresponds to the predicted "thickened flames" for Ka > 1 (Klimov-Williams criterion).

This tendency is contradictory to previous experimental results [15, 16], in which the flame structure with thickened flame front has not observed in instantaneous images. In our measurements, there is ambiguity to determine the mean angle of the instantaneous flame front to the mean flame surface. Also, assuming that there exists the flames with distributed reaction zone which has partially reacting gases, our method may not be valid because the lower peak value is omitted when we obtain the reaction zone thickness. However, its thickness becomes larger by taking partially reacting gases into consideration. Thus, it could be concluded that the thickened flame structure appears in highly turbulent condition, which may have distributed reaction zone.

CONCLUSIONS

We have investigated the premixed flame structure in highly turbulent flow with a cyclone-jet combustor. With Mie scattering imaging, we have obtained tomographic images of flames. The local flame characteristics have been examined with an electrostatic probe. In addition, the new approach has been proposed to determine the reaction zone thickness statistically.

As the turbulence is relatively low, one flame sheet wrinkles and a typical wrinkled laminar flame is formed. As the exit velocity is further increased, the flame wrinkling is increased, but the size of its wrinkles becomes smaller with many cusps on the flame front. When the velocity exceeds 30 m/s, one continuous flame sheet cannot be sustained and PDF of ion current becomes the so-called normal distribution (Gaussian distribution). The statistically obtained reaction zone thickness becomes wider as the exit velocity is increased. From these results, it seems that the destruction of laminar flame structure occurs in highly turbulent combustion and thickened flame structure appears.

REFERENCES

1. G. Damkoehler, Z. Elektrochem. 46, 1940, pp. 601-626.

2. D. R. Ballal and A. H. Lefebvre, Proc. R. Soc. Lond. A. 344, 1975, pp.217-234.

3. M. Summerfield, S. H. Reiter, V. Kebely, and R. W. Mascolo, *Jet Propulsion* 25, 1955, p.377.

4. K. N. C. Bray, *Turbulent Reacting Flows, Topics in Applied Physics*, 1980, Vol.44, pp.115-183.

5. R. Borghi, in Recent Advances in Aeronautics Science, 1985, pp.117-134.

6. N. Peters, *21st Symp. (Int.) on Comb.*, 1986, pp.1231-1250.

7. A. Yoshida, *22nd Symp. (Int.) on Comb.*, 1988, pp.1471-1478.

8. J. Furukawa, E. Harada, and T. Hirano, *23rd Symp. (Int.) on Comb.*, 1990, pp.789-794.

9. A. Yoshida, M. Narisawa, and H. Tsuji, *24th Symp. (Int.) on Comb.*, 1992, pp.519-525.

10. A. Yoshida. and K. Sakurai, *Transport Phenomena in Combustion*, 1995, pp.509-520.

11. T. W. Lee and A. Mitrovic, *26th Symp. (Int.) on Comb.*, 1996, pp.455-460.

12. Furukawa, J., Maruta, K., Nakamura, T., and Hirano, T., *Combustion Sci. Technol.* 90: 267-280 (1993).

13. Bedat, B. and Cheng, R. K., *Combustion and Flame* 100: 485-494 (1995).

14. R. K. Cheng, I. G. Shepherd, B. Bedat, and L. Talbot, *Combustion Sci. and Technol.* (1999), in press.

15. A. Buschmann, F. Dinkelacker, T. Schafer, and J. Wolfrum, *26th Symp. (Int.) on Comb.*, 1996, pp.437-445.

16. M. S. Mansour, N. Peters, and Y. C. Chen, *27th Symp. (Int.) on Comb.*, 1998, pp.767-773.

17. Y. Onuma, M. Morikawa, T. Takeuchi, and S. Noda, *Transport Phenomena in Combustion*, 1995, pp.509-520.

18. K. Yamamoto, T. Achiha, and Y. Onuma, *AIAA Paper*, 2000-0186, 2000, in press.

19. K. Okamoto, J. Furukawa, and T. Hirano, *Nensyo no Kagaku to Gijutsu*, vol.6, 1998, pp.45-53.

20. I. Gokalp, *Combust. Flame* 67:111-119 (1987).

21. Bray, K., N. C., Moss, J. B., and Libby, P. A., *Combust. Flame* 61:127-142 (1987).

22. S. S. Shy, R. H. Jang, W. K. I., and K. L. Gee, *26th Symp. (Int.) on Comb.*, 1996, pp.283-289.

23. I. Yamaoka and H. Tsuji, *20th Symp. (Int.) on Comb.*, 1984, pp.1883-1892.

24. Chew, T. C., Bray, K. N. C., and Britter, R., *Combust. Flame* 80:65-82 (1990).

(Figure Caption)

Figure 1. Cyclone-jet combustor.

Figure 2. (a) Direct photograph, (b) tomographic image of a flame, and (c) axial mean ion current distribution, (U_m = 10 m/s, ϕ_m = 0.75).

Figure 3. Tomographic images of flames in a cyclone-jet combustor, ϕ_m = 0.75, (a) U_m = 10 m/s, (b) U_m = 15 m/s, (c) U_m = 30 m/s.

Figure 4. Signal waveform of ion current, ϕ_m = 0.75.

Figure 5. PDF of ion current, ϕ_m = 0.75.

Figure 6. Signal waveform of ion current and reaction variable, (U_m = 15 m/s, Z = 20 mm, ϕ_m = 0.75).

Figure 7. Radial distribution of probability of reaction zone existing, p, (U_m = 15 m/s, Z = 20 mm, ϕ_m = 0.75).

Figure 8. Reaction zone thickness obtained in this study.

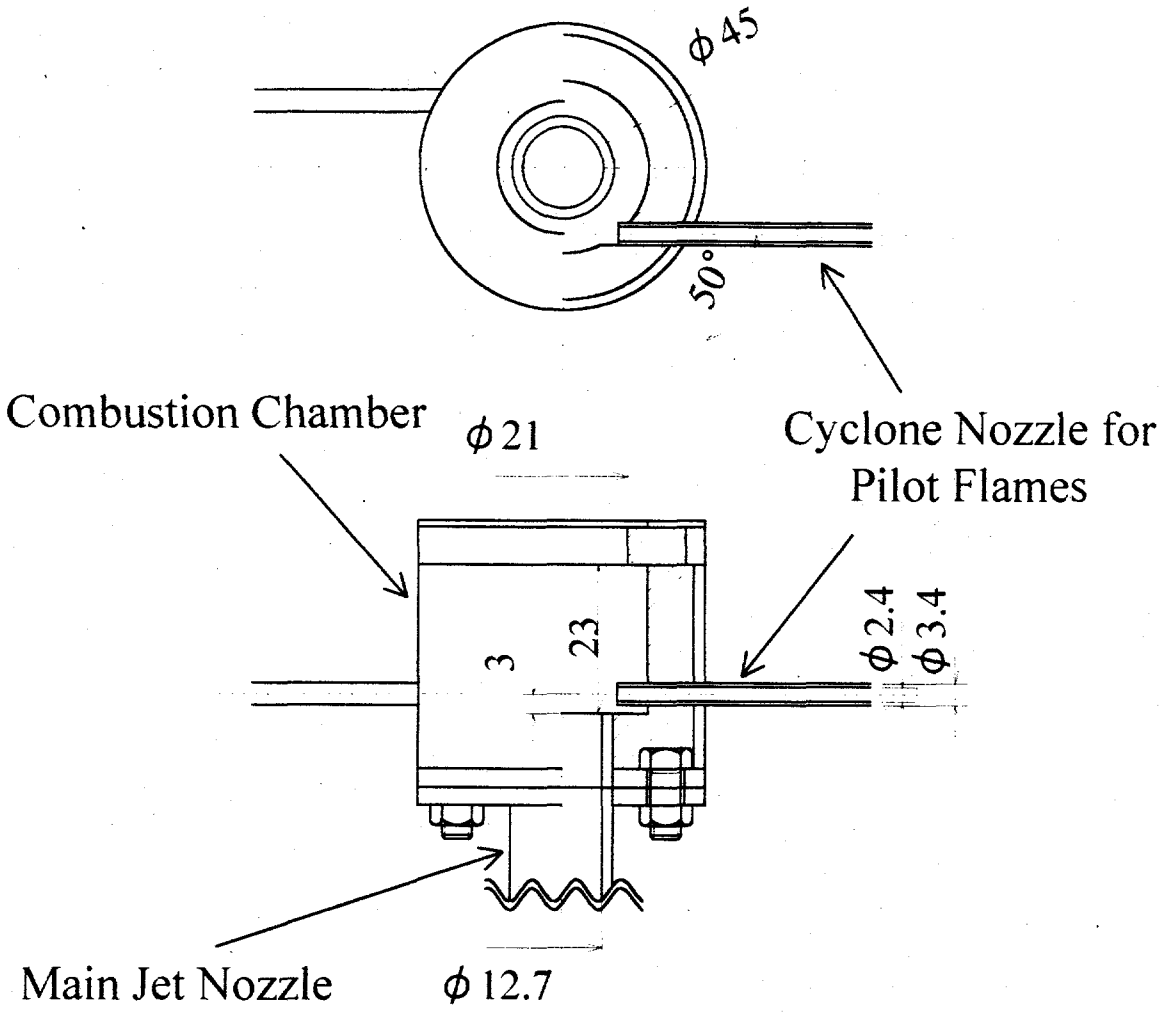

Fig. 1. Cyclone-jet combustor.

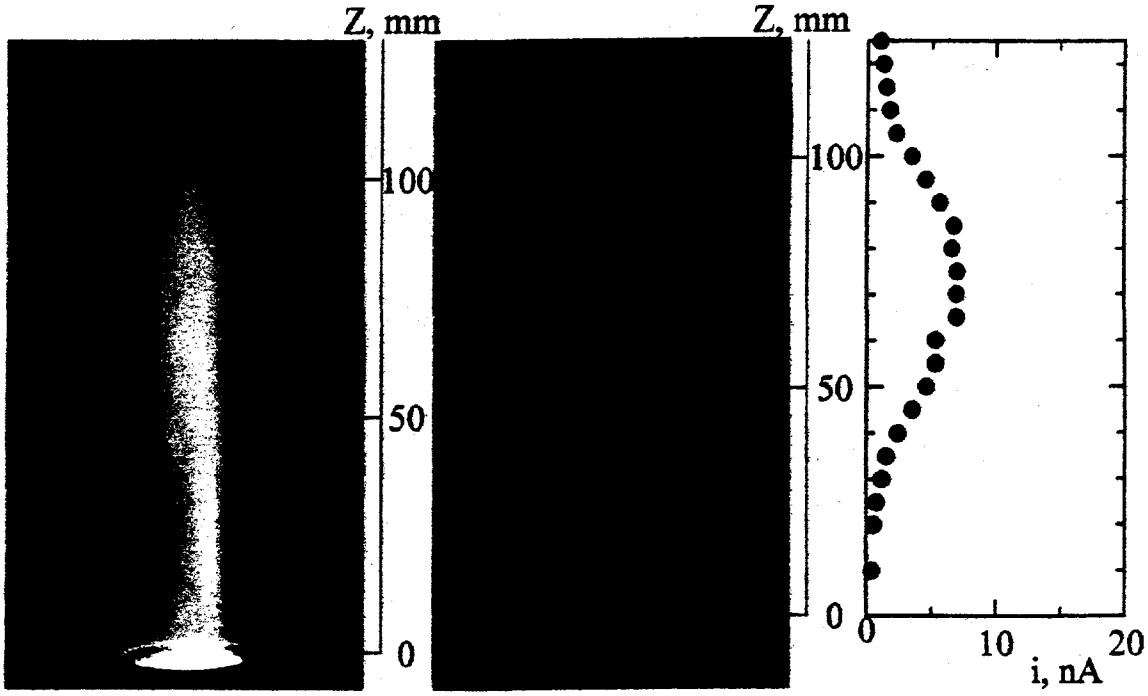

Fig. 2. (a) Direct photograph, (b) tomographic image of a flame, and (c) axial mean ion current distribution (U_m = 10 m/s, Φ_m = 0.75).

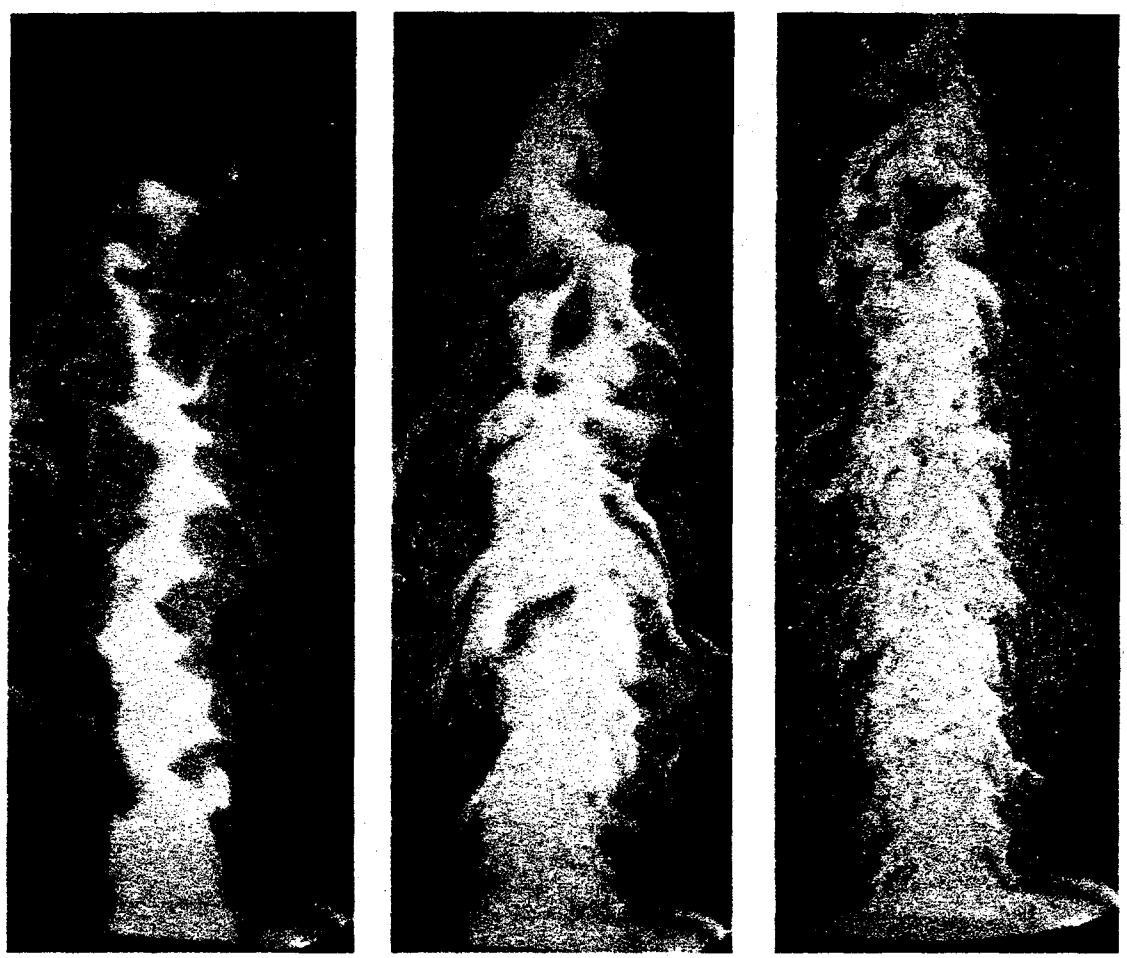

(a) (b) (c)

Fig. 3. Tomographic images of flames in a cyclone-jet Combustor, $\Phi_m = 0.75$, (a) $U_m = 10$ m/s, (b) $U_m = 15$ m/s, (c) $U_m = 30$ m/s.

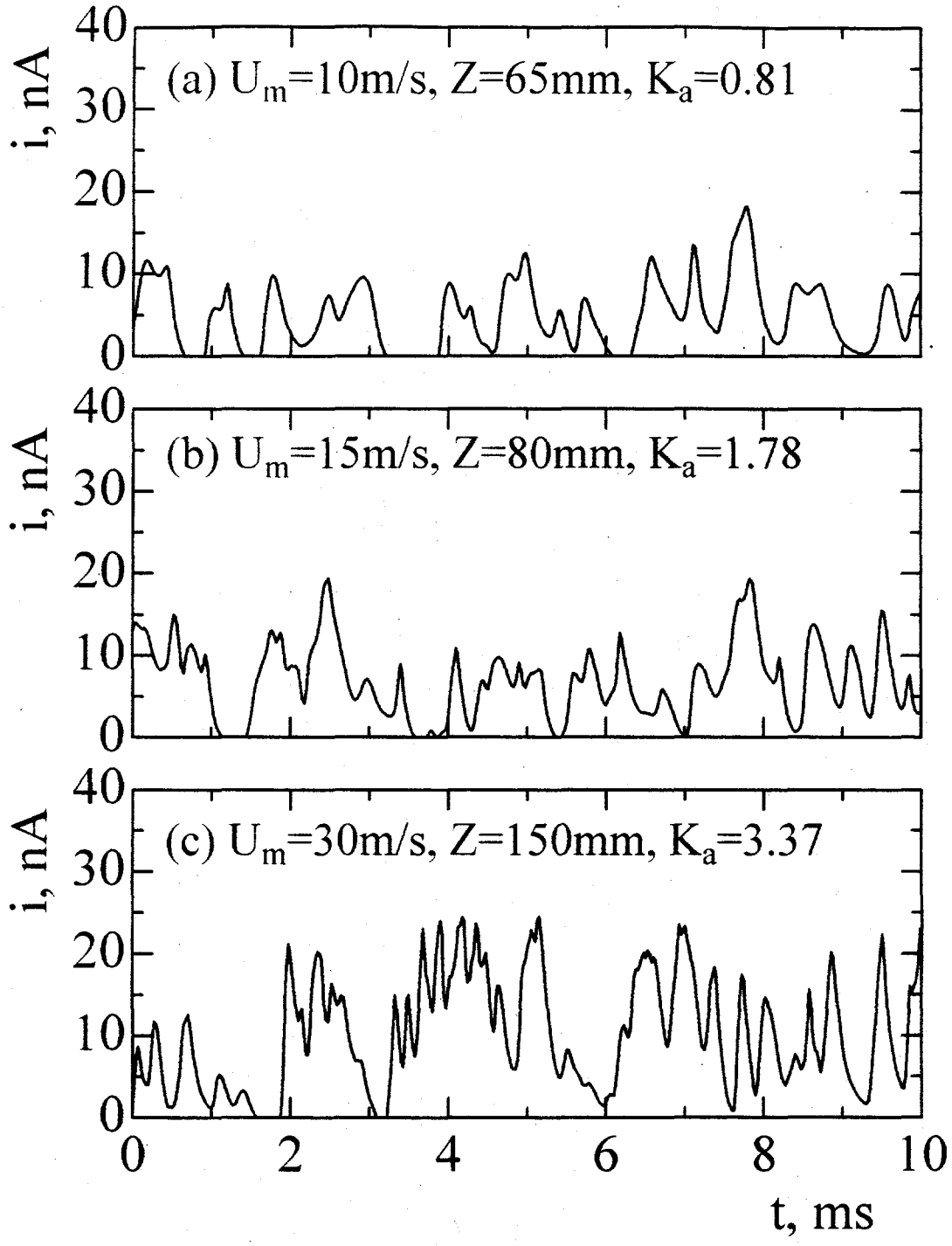

Fig. 4. Signal waveform of ion current, Φ_m=0.75.

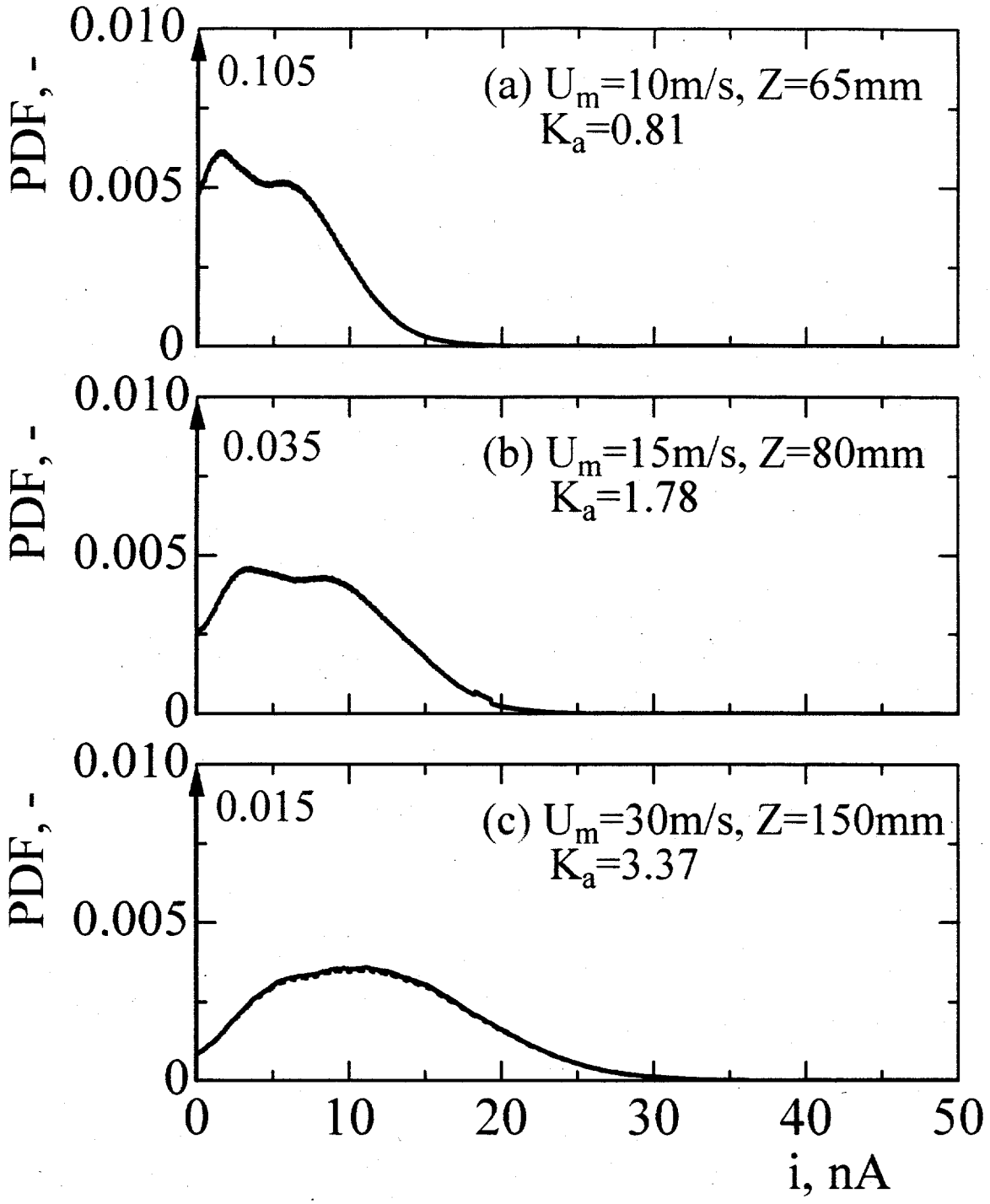

Fig. 5. PdF of ion current, Φ_m=0.75.

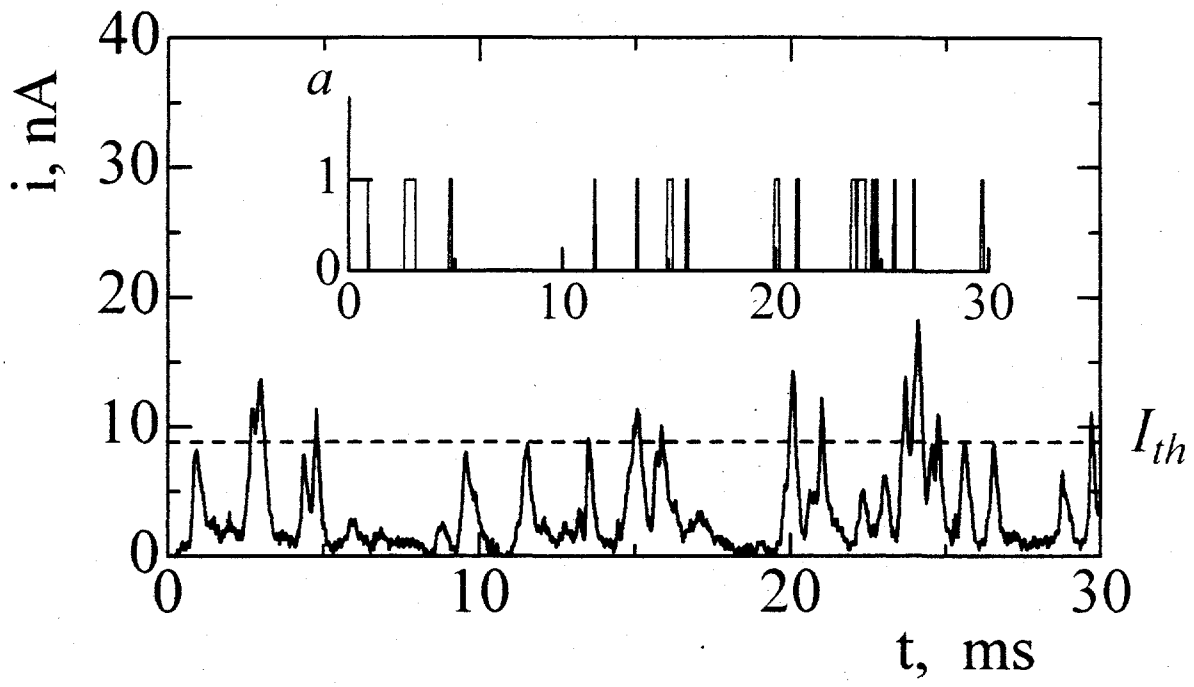

Fig. 6. Signal waveform of ion current and reaction variable, (U_m=15m/s, Z=20mm, ϕ_m=0.75).

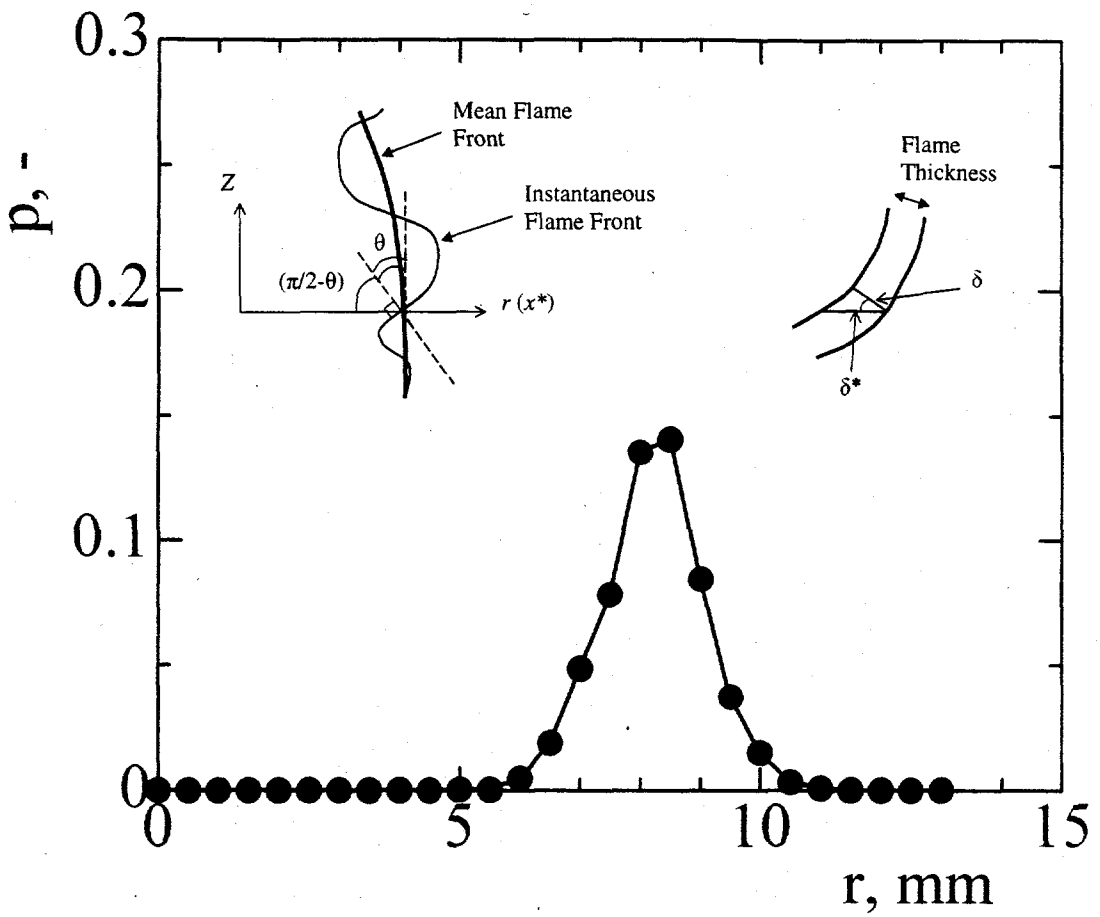

Fig. 7. Radial distribution of probability of reaction zone existing, p, (U_m =15m/s, Z= 20mm, ϕ_m=0.75).

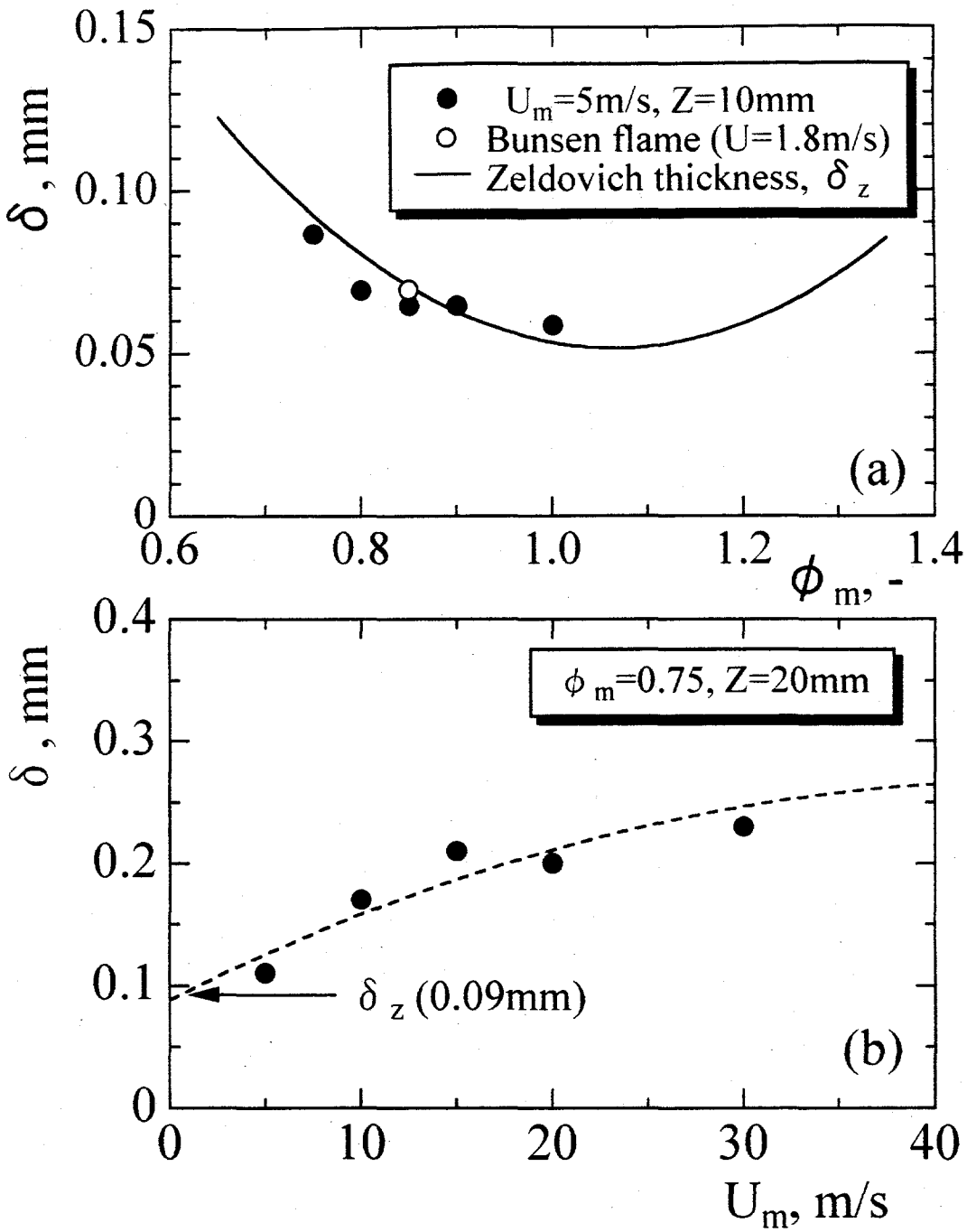

Fig. 8. Reaction zone thickness obtained in this study.